PROJECT DESCRIPTION

1. PROPOSAL OVERVIEW

The goal of this proposal is to study the role of synaptic ensheathment (the tightness of wrapping of the synapse by astrocytes) in regulating the spiking activity of the network. It is now known (and reviewed in Section 2.3 below) that the synaptic ensheathment properties vary considerably between the brain areas and also in some disease conditions (such as epilepsy and Alzheimer's). However, what role that might play in regulating the brain activity is unknown. This is the question we set out to investigate.

We are particularly **motivated** by preliminary indications from our collaborator Wilcox's lab that the synaptic ensheathment might be enhanced during epilepsy in hippocampal CA3-CA1 network. Such changes might be contributing to the run-away excitability and to seizures, or, conversely, they might be playing a compensatory, protective role. We will use computational modeling and mathematical analysis at different spatial scales to differentiate between these two options. Importantly, the approaches that we choose to employ are quite general, and the results will be relevant to other networks and experimental situations as well. For example, in our collaborator White's lab, they are attempting simultaneous recordings from neurons and astrocytes, and having better theoretical understanding of their interactions would help formulate predictions and plan future experiments.

1.1 Intellectual merit

Astrocytes are newly recognized crucial contributors to brain function and dysfunction. They are roughly as numerous as neurons in the mammalian brain and serve a number of critical roles. Perhaps surprisingly, there is relatively little known about specifics of their interaction with neurons. Expected findings from this work will contribute to understanding of the complex interactions between the two major brain cell types.

Synaptic ensheathment, one of the main themes in this proposal, is ubiquitous in the brain, but it is not ordinarily included in models as a property of network structure. Thus, this study explores a novel aspect of a more general problem of *network structure-function* relationship, central in modern neuroscience.

Notably, this study is truly *multiscale*. We will first study the influence of degree of synaptic ensheathment on the synaptic function at the fine spatial scale and short time scale of molecules and receptors. Then we will look at the still detailed level of an individual synapse. But, crucially, based on our detailed studies, we will derive a network-level way to include synaptic ensheathment. To be useable in a wide variety of networks, this network-level description needs to be minimal, for ease of implementation and minimization of computing costs. We will provide a straightforward way to include the degree of synaptic ensheathment among the properties of an idealized synapse, often used in spiking neuronal networks.

As explained below in Sec. 4, development of detailed biologically-based models and computer simulations will play an important role in the proposed work. We also propose to develop *new mathematical tools*: extending analysis of diffusion with switching boundaries to spatially-extended initial conditions (Sec. 4.1); extending a method to quantify roles of individual parameters in controlling the system behavior (Sec. 4.2); and extending the network activity coherence measures to include synaptic ensheathment (Sec. 4.3).

The work will be undertaken in Dr. Borisyuk's group at the Department of Mathematics, University of Utah. Professor Borisyuk is an expert in computational modeling in neuroscience. She has an active research group that is involved with both Mathematical Biology community in her department, and the Neuroscience program. Dr. Borisyuk has a history of successful collaborations with both mathematicians and biologists, and this project involves such collaborations as well. We plan to recruit a graduate student to be involved in component I of the project; another graduate student to develop models for component II of the project in consultations with collaborator White; and a postdoctoral researcher to be involved in all aspects of the project, but focusing particularly on component III.

1.2 Approach

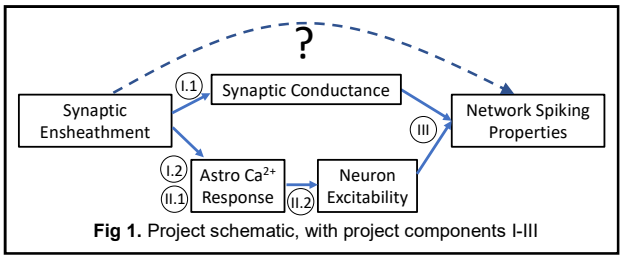

Fig 1. Project schematic, with project components I-III

We will approach the question about the relationship between synaptic ensheathment and network firing properties in three distinct project components (Fig. 1) described in detail in Section 4. The project components I and II will uncover the specific relationship between the degree of ensheathment (S) and the properties of individual synapse. Namely, we will show how S affects the (random) number of molecules reaching the post-synaptic (I.1) and astrocytic (I.2) receptors as a function of time, the resulting astrocyte calcium response (II.1), and excitability of the postsynaptic cell (II.2). As a result, we will obtain from detailed biologically-realistic studies, synaptic and post-synaptic properties as parametrized by S. In the project component III we will consider an excitatory-inhibitory network, with each synapse endowed with its ensheathment parameter, and thus its own properties. We will then ask how the distribution of the synaptic ensheathment parameter in the network relates to its firing rate and synchronization properties.

2. BACKGROUND

2.1 Astrocytes in the mammalian brain

Astrocytes are the major glial cell type in the mammalian brain (Verkhratsky *et al.*, 2012). With the advancement of experimental technologies (transgenic mice and Ca^{2+} imaging), studies have revealed that astrocytes play many key roles in the central nervous system (CNS). Astrocytes have been shown to be involved in the uptake of neurotransmitters (e.g. glutamate and GABA) (Anderson and Swanson, 2000; Zhou and Danbolt, 2013), gliotransmission (release of neuroactive compounds such as glutamate, ATP) (Bezzi *et al.*, 1998; Newman, 2003; Liu *et al.*, 2005; Wang *et al.*, 2013), K^+ buffering (Wallraff, 2006; S. Wang *et al.*, 2012; Larsen *et al.*, 2014), and regulating the blood-brain-barrier (Verkhratsky *et al.*, 2012).

Through such functions, astrocytes are able to modulate neuronal activity at the level of a single synapse as well as in large neural networks. Astrocytes are thought to be involved in synaptic plasticity, learning, memory and some CNS disorders. For instance, astrocytes undergo morphological and functional changes in epilepsy (Stewart *et al.* 2010), Huntington's disease (Tong *et al.* 2014), and Alzheimer's disease (Mattson and Chan, 2003; Orr *et al.*, 2015), which could lead to changes in neuronal function. Also, astrocytes have been shown to contribute to long-term potentiation (LTP) and long-term depression (LTD) in hippocampus (Gerlai *et al.*, 1995; Khakh and Sofroniew, 2015), neocortex (Pankratov and Lalo, 2015), and cerebellum (Shibuki *et al.*, 1996). Moreover, studies have proposed that astrocytes are involved in modulating various brain rhythms, such as gamma (Sakatani *et al.* 2008) and theta (Parpura and Haydon, 2009).

2.2 Previously studied pathways of astrocyte-neuron interactions

In view of this experimental evidence, neuronal synapses are sometimes viewed as tripartite: neuron activity modulates astrocytes, with feedback onto the neuron (Araque *et al.*, 1999). However, the exact mechanism that enables astrocytes to provide feedback to the pre- and post-synaptic terminals is still under investigation. Gliotransmission, the act of astrocytes releasing vesicle-dependent neurotransmitters when their intracellular calcium is elevated, is one hypothesis favored by some experimentalists and modelers, despite the controversies surrounding this mechanism. One can find experimental papers supporting (Pascual *et al.*, 2005; Schwarz *et al.*, 2017; Covelo and Araque, 2018) and openly questioning the existence of such mechanism (Haydon and Nedergaard, 2015; Chai *et al.* (2017); Fiacco and McCarthy, 2018).

In fact, the majority of mathematical model that have investigated the full astrocyte-neuron interaction assume that astrocytes affect neurons only through gliotransmission. Specifically, such models have shown that through gliotransmission, astrocytes may be able to change the firing patterns of nearby neurons (Di

Garbo *et al.*, 2007; Wade *et al.*, 2011), alter the induction of LTP and LTD (De Pittà and Brunel, 2016), and have consequences for the overall network behavior (Amiri *et al.*, 2012; Reato *et al.*, 2012).

However, gliotransmission is not the only suggested pathway for astrocytes to modulate neuronal networks. Elevated intracellular calcium may drive sodium-calcium exchangers (NCX) and the sodium-potassium pumps (NKA) to pump potassium into the cell, thus decreasing the extracellular potassium concentration, and changing the resting potential for nearby neurons (Wang *et al.*, 2012). It has also been proposed that astrocytic long-lasting potassium current mediated by Kir4.1 channels (inward-rectifying K^+ channels expressed in astrocytes) may also affect nearby neuronal activity through the extracellular potassium concentration changes (Sibille *et al.*, 2014).

These pathways may all be mediated via calcium transients. Activation of surface receptors leads to increases in intracellular Ca^{2+} in astrocytes through several pathways, including one in which the signaling molecule inositol (1,4,5)-trisphosphate (IP_3) serves as an intermediary. Furthermore, astrocyte Ca^{2+} elevations can propagate through multiple segments of one astrocyte or between astrocytes (Haydon, 2001), providing a method for inter- and intracellular communication. Despite significant research efforts, there is little consensus on the role of astrocyte calcium signaling in the brain. Until recently, there were no experimental techniques that could track changes in Ca^{2+} concentration with sufficient spatial and temporal resolution to accurately assess astrocyte function. Concomitant with this lack of experimental data, the modeling of astrocytic Ca^{2+} transients is lagging behind similar work in neurons.

Parts of the astrocyte signaling pathways have been investigated with mathematical models. Those that have focused on calcium transients, have assumed that the calcium release is triggered through IP_3 molecule. The modeling has shown that astrocytes may be able to convey signal information via frequency or amplitude of calcium oscillations (De Pittà *et al.*, 2009), that IP_3 diffusion may mediate the synchronization of calcium oscillations in neighboring astrocytes (Ullah et al., 2006), and that receptor stochasticity may play an important role in calcium response variability (Toivari *et al.*, 2011). It is important to note, however, that latter two models were created in reference to highly idealized experimental condition of bath application of agonists to cultured astrocytes, while De Pittà *et al.* (2009) includes a closed-cell assumption, i.e. assumes that the total calcium level inside an astrocyte is constant.

Other models have considered the role of either astrocyte potassium buffering or glutamate uptake on neuronal activity, while omitting the astrocyte calcium dynamics. (Wei et al., 2014) accounted for astrocytic influences on nearby neurons by modeling extracellular potassium concentrations. Scimemi *et al.* (2009) and Allam *et al.* (2012) models allowed for detailed diffusion of glutamate within the synaptic cleft, and suggested that astrocytes play an active role in synaptic plasticity via glutamate uptake. Further, Sibille *et al.* (2015) specifically modeled potassium uptake in astrocytes by including the Kir4.1 channel and NKA, and explicitly showed that potassium uptake in astrocytes had the ability to regulate neuronal excitability. None of these models, however, include detailed description of astrocyte calcium dynamics.

2.3 Astrocytic ensheathment of the synapse

So, while models exist that have examined some of the possible pathways through which astrocytes can modulate neuronal behavior, no model has investigated how these pathways may be interacting with each other. This interaction may be subtle, while also critically important, and in order to study it sufficiently, one must also include the astrocyte's ability to *ensheath*, or tightly wrap around, the synapse. Interestingly, this concept has not been included in previous mathematical studies, where they have assumed the astrocyte portion of tripartite synapses does not vary from synapse to synapse. However, experimentally, it has been shown that the number of synapses ensheathed by astrocytes is usually well below 100%, and can differ dramatically between brain regions (e.g. 74% of cerebellar Purkinje cell synapses, 29% of the dendritic

spines in the mouse visual cortex, and 60% of hippocampal synapses are ensheathed (Špaček, 1985; Ventura and Harris, 1999)). To complicate matters further, these synaptic ensheathment measurements are done via fixed-tissue electron microscopy, and do not capture dynamic changes to levels of ensheathment (Murphy-Royal *et al.*, 2017), with a notable exception of studies in endocrine regulation (Tasker *et al.*, 2012). It is not hard to imagine that the proximity of an astrocyte's processes to a synapse could easily affect all of the major pathways of astro-neural interaction mentioned previously, and so a complete understanding of these pathways, and how they may interact with one another, is incomplete without accounting for synaptic ensheathment by astrocytes. Further, disease states such as epilepsy and Alzheimer's disease are known to have an increased number of hypertrophic astrocytes, known as reactive astrocytes (Coulter *et al.*, 2015; Heneka *et al.*, 2015). While reactive astrocytes vary in a number of ways from non-reactive astrocytes, their swollen structures imply a much tighter level of ensheathment. Thus, in order to understand how reactive astrocytes may affect the brain in these disease states, we much first investigate the more basic research problem of how astrocyte ensheathment of synapses affects baseline neuronal activity.

In order to investigate the role of astrocyte ensheathment at the network level and to relate this work to that of existing literature, we need to use and extend the tools already used to link network structure properties with the neural firing characteristics. It is well known that pairwise spike train correlations can yield the full statistical structure of neuronal network firing, and a wealth of theoretical work has been extended from this key observation (Schneidman *et al.*, 2006; Shlens *et al.*, 2006; de la Rocha *et al.*, 2007; Shea-Brown *et al.*, 2008; Ocker *et al.*, 2017). In our study we will focus on a two-layer network, with a layer of feedforward neurons, and a layer of recurrent neurons (similar to how CA3 area of hippocampus projects onto CA1 area). A recent paper by Rosenbaum *et al.* (2017) showed how the width of connectivity profiles, in the feedforward and recurrent layers, determine the ability of a network to synchronize. Specifically, by performing mathematical analysis in the limit of large network size, they found the network was able to maintain an asynchronous state only when the radius of the recurrent projections is less than that of the feedforward ones. Thus, there are important advances being made in connecting the structure properties of the networks with the network firing, but this field of work has not included astrocytes into consideration.

3. PRELIMINARY STUDIES

3.1. Astrocyte calcium modeling

In recent work, we investigated evoked calcium transients in coronal brain slices from mice with a mathematical model (Handy *et al.*, 2017; Taheri *et al.*, 2017). (This work was done in collaboration with John White's lab, who is also a collaborator on this proposal, and partially supported by the NSF DMS-1022945 and DMS-1148230). Fig. 2A shows a simplified schematic of the Ca^{2+} activity components in our model. The model input is a transient increase in IP_3 concentration (the increase is due to agonist binding to membrane receptors, but this process is not included in the model). IP_3 then binds to IP_3 receptors (IP_3Rs) on the endoplasmic reticulum (ER) membrane, which consequently opens IP_3R channels and allows Ca^{2+} to enter from ER to the cytosol. When there is significant depletion of Ca^{2+} from the ER, store operated Ca^{2+} (SOC) channels are activated, and allow for additional Ca^{2+} flow from the extracellular space (ECS) into the cytosol. Sustained, elevated levels of cytosolic Ca^{2+} inactivate IP_3Rs, and activate sarco/endoplasmic reticulum Ca^{2+} ATPase (SERCA) pumps and plasma membrane Ca^{2+} ATPase (PMCA) pumps, which then transfer the cytosolic Ca^{2+} back to the ER and ECS, respectively. After the degradation of IP_3, these pumps and channels return the system to steady state.

Experimentally, our collaborators applied brief (16–250ms) local pulses of ATP and examined Ca^{2+} responses in three subcompartments of imaged astrocytes: the soma, large, and small processes. In the data, we observed variability among simultaneous responses of different cells and different subcompartments within a cell, and between trials in a given subcompartment. Even when agonists are bath applied and the

spatial variability of the agonist is reduced, responses in different cells or astrocyte subcompartments vary greatly in their shapes and durations (Xie *et al.*, 2012). It therefore became our goal to develop a mathematical model that generates Ca^{2+} responses with a variety of temporal features, similar to those seen experimentally, to understand the underlying dynamical system governing these behaviors, and to use the model to examine the sources of response variability.

In order to quantify diversity in astrocyte Ca^{2+} signaling, we divided all Ca^{2+} responses into four main categories according to their shape and duration: Single-Peak (SP), Plateau (PL), Multi-Peak (MP), and Long-Lasting (LL). Fig. 2B, first column shows example traces of cytosolic Ca^{2+} elevations elicited by 30–63ms applications of ATP, while the second column shows a stereotypical response for each class, generated by our model, chosen to match the experimental responses in the first column. This response type categorization is based on our data, the mathematical structures underlying our model dynamics, and the astrocyte literature (Verkhratsky and Kettenmann, 1996; Xie *et al.*, 2012; Bonder and McCarthy, 2014).

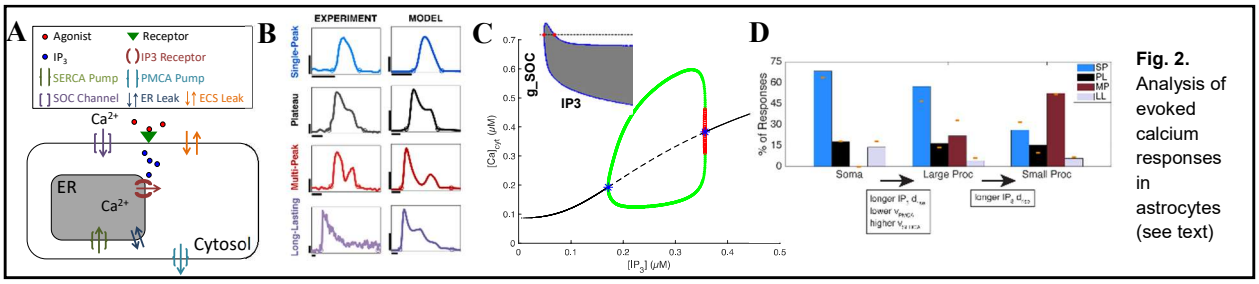

Fig. 2. Analysis of evoked calcium responses in astrocytes (see text)

Specifically, we elucidated the mathematical structures underlying the above-described dynamics, by treating IP_3 as a bifurcation parameter and examining the smaller three-dimensional system consisting of only cytosolic calcium, the total amount of free calcium in the cell, and the activation variable related to the IP_3R. The bifurcation diagram of this subsystem can be seen in Fig. 2C (black is the steady state; solid=stable, dashed=unstable). As illustrated in this figure, a supercritical Hopf bifurcation occurs at $[IP_3] \approx 0.18$ μm (black asterisk 1) that causes the single stable steady state to transition into a stable limit cycle (max and min of the cycle are shown in green). This stable limit cycle is eliminated by an unstable limit cycle (red) originating at a subcritical Hopf bifurcation at $[IP_3] \approx 0.35$ μm (black asterisk 2).

With this diagram in mind, one can visualize how a stereotypical SP, MP, and PL response is generated if the IP_3 transient has a much slower timescale than the rest of the system. Due to the excitability of the IP_3R, a large enough IP_3 transient produces an initial calcium response. If the amplitude of the IP_3 transient is small enough (below the supercritical Hopf point), the calcium levels simply return to steady state, generating an SP response. On the other hand, if the IP_3 transient amplitude goes beyond this first bifurcation point, we are placed in the oscillatory regime, and if IP_3 remains elevated long enough, an MP response is generated. Lastly, if the IP_3 transient amplitude goes past the second bifurcation point, the calcium levels land on the higher steady state before decaying back to baseline; thus, a PL response is generated.

Note that the above analysis is idealized, since IP_3 in our simulations is not always slower than the rest of the system. However, this general framework proved useful in understanding and categorizing of basic calcium response types based on underlying dynamic structure. Further, we investigated the changes to dynamics under various biologically relevant conditions, such as pharmacological blocking of individual currents, making specific experimentally-testable predictions. Some of these predictions were made by generating and analyzing bifurcation diagrams for corresponding parameter conditions. For example, two-parameter (IP_3 vs. strength-of-SOC) diagram is shown as an inset to Fig. 2C (grey is oscillatory, white is stable steady state region; dashed line – same parameter values as the main bifurcation diagram). Using it,

we predicted that upon partial blocking of SOC channels the oscillatory (MP) responses will become more common, but upon complete blocking of these channels, the multi-peak response will be fully eliminated.

Next, we used our understanding of the parameter space to create a database that can be used by experimentalists to help determine the underlying, experimentally inaccessible calcium-handling mechanisms in their cells. This database, as well as all of the corresponding code for these papers, has been uploaded to ModelDB (Hines *et al.*, 2007) (Model no. 189344). We used the database to match our collaborators' experimental data from different astrocyte compartments. Fig. 2D shows how often each response type is observed (bars=model, orange ticks=data). By comparing the locations of the data matches in the database, we predicted that (i) large processes include IP_3 dynamics with longer rise durations, and (ii) the Ca^{2+} flux rates through the PMCA and SERCA pumps are, respectively, lower and higher in the large processes than the soma. The small processes' profile can be generated by increasing IP_3 rise durations even further, but using the same Ca^{2+} flux parameters as for large processes.

3.2. Mathematical analysis of the diffusion with recharging receptors at the boundary.

In collaboration with Dr. Sean Lawley (Math, Utah) we have recently considered the interaction of neurotransmitter with receptors in the synaptic cleft – a stochastic process we termed DiRT (diffusion with recharging traps). This work was partially supported by NSF DMS-1148230. Mathematically speaking, the setup involves a finite number of particles diffusing in a bounded domain (these are the neurotransmitter molecules that have been released by the presynaptic cell), Fig.3A. Eventually, each particle will leave the domain through either an *escape* region in the boundary (absorbing boundary; dashed) or a *capture* region in the boundary (a switching part of the boundary corresponding to a receptor; red). After a receptor captures a particle, it cannot capture additional particles until after a positive *recharge* time (Fig. 3B). The concept of recharge time stems from the conformational change by the receptor after particle capture. We found that this recharge time can dramatically reduce the number of particles that are captured before they escape. (Note that the same mathematical results apply in a more general context of many biological processes, including hunting by ambush predators, but it is the synaptic interpretation that is relevant here).

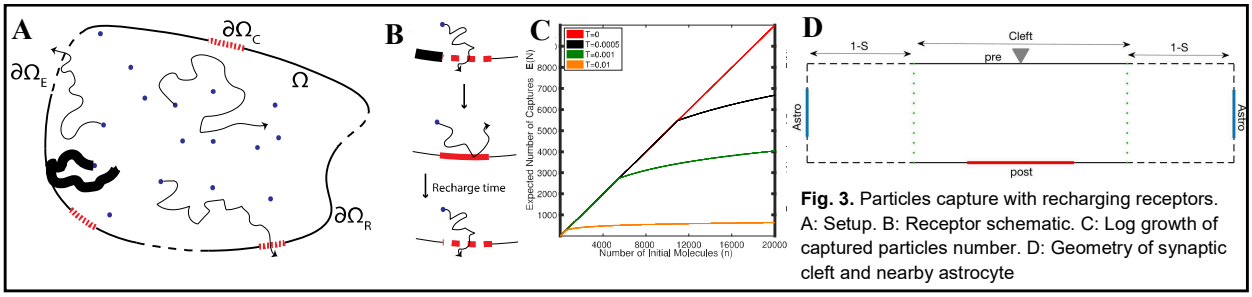

Fig. 3. Particles capture with recharging receptors. A: Setup. B: Receptor schematic. C: Log growth of captured particles number. D: Geometry of synaptic cleft and nearby astrocyte

We proved (Handy et al., 2018a), through a series of lemmas and theorems, that when the recharge time is positive, the expected number of captured particles ($\mathbb{E}[N]$) is bounded from above by the expression:

$$\mathbb{E}[N] \leq \min\left\{m + \frac{m}{T}\log^+\left(C\frac{nT}{m}\right) + \min\left\{nC, \frac{m}{T}\right\}, hn\right\},$$

where m is the number of receptors, n is the initial number of particles, T is the relative recharge time, h is the probably of hitting a receptor, and C is a constant that depends only on the initial distribution of particles, the domain, and the size of the escape regions. This upper bound highlights the importance of including the non-zero recharge time into consideration: if the capture regions recharge instantly *(T=0)*, then the expected number of captured particles grows linearly in n; however, for all $T > 0$ the linear growth can only hold for $n<n_c$, where n_c is determined by:

$$m + \frac{m}{T}\log^+\left(C\frac{n_c T}{m}\right) + \min\left\{n_c C, \frac{m}{T}\right\} = hn_c.$$

In Fig. 3C we plotted the upper bound as a function of n for different values of T. As T increases, the upper bound branches off of the linear instant recharge case (red line) at smaller values of n. While the statements above provide logarithmic upper bounds for *E[N]*, we confirmed in Monte Carlo simulations that the actual expected number of captured particles does grow logarithmically (and not sub-logarithmically).

We have also shown (Handy, Lawley and Borisyuk, 2018b) that the coefficient of variation of *N* for the process with recharge is always higher than the instantaneous process, meaning that it has increased variability. We also find that the recharge rate determines the mean and variance of the clearance time, defined as the time it takes for all particles to leave the domain. The clearance time is also affected by the size of the domain, but is quite insensitive to the number of receptors. We also extended the model to partially absorbing traps (a particle that comes in contact with a capture region has some probability of not being captured) by including an appropriate Robin boundary condition, and find that the domain size and number of traps, respectively, control the duration and amplitude of the trap activation.

Importantly, while insight into this problem can be gained with direct Monte Carlo simulations of the DiRT process, such simulations are computationally expensive for a large number of particles. Further, due to the correlations that arise between particles, this spatial and stochastic process is challenging to investigate analytically. Thus, we developed new tools by approximating this stochastic process with a continuous-time Markov process on a discrete state space, along with its corresponding mean field approximation and reduction in the limit that captures occur instantly. The Markov process has the following transitions,

$(P,C,R) \rightarrow (P\text{-}1,C,R)$ at rate γP | $(P,C,R) \rightarrow (P,C,R+1)$ at rate $\rho(m-R)$ | $(P,C,R) \rightarrow (P\text{-}1,C+1,R\text{-}1)$ at rate $\upsilon PR/m$

where *P(t)* is the number of particles in domain at time *t*, $C(t)$ is the number of captures before time *t*, and $R(t)$ is the number of available receptors. The transition rates include the escape rate γ, recharge rate $\rho=1/T$, and capture rate υ, which can be estimated for each domain geometry (see algorithm in Handy *et al.*, 2018b).

3.3. Results from prior NSF support.

NSF-DMS DMS-1148230; RTG: Research Training in Mathematical and Computational Biology; Amount: $2,496,299; 08/01/12-07/31/19; Alla Borisyuk's role: co-PI.

This grant supports a comprehensive program of cross-disciplinary research and training in Mathematical and Computational Biology, in the Math Department of the University of Utah. The goal of this program is to train fully integrated, collaborative researchers and scholars in mathematical and computational biology, thus bringing to bear the power of mathematics on the challenging problems of modern biology.

Intellectual merit. To date, the program has recruited a strong and diverse group of 32 graduate students. Most of them were funded for two early semesters and could apply for funding in later years, and also spend a summer in an experimental lab, getting immersed in the biological culture and fostering collaborations. Students are encouraged to have a biologist on their thesis committee. In addition to research, students participate in journal club (led by an advanced RTG student and a postdoc, they critically analyze modern and classical papers), group meetings (with feedback on their presentations), seminar de-briefings, retreats, seminar, professional development events. As of Fall 2018, 13 students received their Ph.D.'s, with more preparing to defend this year. All of the graduates successfully found jobs of their choice, ranging from academic positions across US to work in local companies. RTG has also contributed to funding 3 postdocs. They receive mentoring on research, teaching, professional development, and are given opportunities to mentor graduate and undergraduate students, and to take on other leadership roles.

The PI of this proposal is advising 4 of the RTG students. For several others she is serving on their thesis committees. Two of the recent research efforts most relevant to this proposal involve RTG student Gregory Handy, and are described in sections 3.1 and 3.2 above. They resulted in four publications (3 published, 1

submitted). Three other papers from PI's group on research partially funded by RTG have also been published or submitted, and other RTG students are preparing their manuscripts for publication. Code, data, and simulation results from these publications are publicly available online in ModelDB or GitHub.

Broader impact. Research conducted by RTG participants has resulted in 87 publications involving RTG students, faculty and postdocs. Numerous talks and posters were presented by RTG participants at various workshops and meetings. For trainees this experience is an integral part of their training and professional development. Several students received poster prizes at conferences such as SIAM Life Sciences and Society for Mathematical Biology meeting.

The grant has contributed partial funding to 17 REUs. Some of these undergrads worked under guidance of a graduate student or a postdoc, providing simultaneous learning and mentoring experience to the trainees.

RTG has been sponsoring an active Math Biology Seminar (10-15 speakers from across US and 5-10 local speakers from various departments yearly). The seminar abstracts and other details are maintained at: http://www.math.utah.edu/research/mathbio/mbseminar/mathbio_seminar.html. The seminar speakers are asked to attend a pre-seminar lunch with graduate students for informal interaction. The seminar serves as a gathering point for quantitatively minded biologists and biology-loving mathematicians.

Having RTG grant on campus has allowed to create a lively, engaged, vertically integrated interdisciplinary community. Many RTG participants are actively involved in outreach activities to public, in local schools, teacher training, etc. Many of the research activities become topics in graduate and undergraduate courses.

4. PROPOSED RESEARCH

We propose to investigate the role of astrocyte ensheathment in neuronal networks, employing multi-scale approaches that span from the diffusion of neurotransmitters to firing properties of a full network model. This study is motivated by specific biological questions. It is expected to advance understanding of possible roles of synaptic ensheathment variability, and generate predictions for future biological experiments. It is also expected to advance theory of stochastic processes (diffusion with randomly switching boundary) and theory of correlations in neural networks activity.

4.1. Molecular scale.

Rationale. In the first part of the project we will look at the spatial scale of the neurotransmitter molecules diffusing in the synaptic cleft. Once a molecule is released, it diffuses until it leaves the synaptic cleft or binds to the receptors on either the postsynaptic neuron (generating postsynaptic conductance) or the astrocyte (leading to astrocyte calcium response via a cascade of reactions).

In the previous work (Section 3.2) we have shown that the fate of the molecules and the binding to receptors depends in specific ways on many parameters, including the receptor "recharge" time, the geometry of the cleft, number and location of receptors, etc. In this first part of the proposal our goal is to extend our results to produce statistics of receptor activation time course as the ensheathment parameter is changed. We need to produce receptor activation profiles separately for the postsynaptic receptor neuron (**Component I.1**), and the nearby astrocyte (**Component I.2**), as their receptors are located in different parts of the domain.

Proposed work.

Component I.1. Neurotransmitter binding to postsynaptic receptors.

(This project component is smaller than the others, is well-defined, and requires minimal background, so it would make a great project for an REU student wishing to learn about diffusion, simulations, and statistics.)

First, the degree of ensheathment S will be included into consideration as a parameter determining the width of the box pictured in Fig. 4 or 3D. The non-ensheathed synapse will have the largest box, then the box size

will decrease with increasing degree of ensheathment. At the highest levels of ensheathment the astrocyte walls will move within the synaptic cleft box marked by green boundaries.

For a fixed S, our previous work (Section 3.2) gives us microscopic description of the molecule motion. In particular, it gives us the mean and the variance of the cumulative number of postsynaptic captures and the the number of available receptors. However, for the subsequent parts of the project we want to generate realizations of the more macroscopic quantity of synaptic conductance as a function of time, consistent with the statistics of the molecules binding. This will be achieved by running molecular simulations of either the original DiRT process, or one of the approximations of Handy et al., (2018b), and accumulating statistics of the time of maximum, amplitude and the decay time of the receptor activation and their changes with S. Having these distributions will allow us to generate valid realizations of the post-synaptic conductance.

We expect that the duration of the conductance should be consistent with our theoretical estimates for the molecules clearance time, and the rise time should relate to time that it takes to arrive at the quasi-stationary distribution of the process (Handy et al., 2018b).

Further, beyond an REU-level project, and more appropriate for a graduate student, our mathematical results need to be generalized to the case of the partially absorbing receptors (defined in Section 3.2), as current theorems only hold for fully-reliable receptors. We also need to ask whether our model can explain why the receptors tend to occur in clusters, and be located across from the release site. For example, these arrangements could give an advantage in terms of variability of the postsynaptic signal. In another important extension we plan to turn a part of the upper reflecting boundary in Fig. 4 into absorbing, to account for recycling of neurotransmitter by presynaptic cell. That change would not alter our fundamental results, such as logarithmic growth in the number of captures, but it might affect, e.g., rise time of the receptor activation.

Component I.2. Neurotransmitter binding to astrocyte receptors. To include astrocyte in our synaptic model we note that if the astrocyte is wrapped around the synapse, it limits the amount of extracellular space available around that synapse. Thus, we can consider that the astrocyte was already included in our previous set up for this problem, playing the role of a part of absorbing domain boundary (Fig. 4 and 3D). There is evidence that because of the high concentration of glutamate transporters on the surface of the astrocyte, it is quite effective at removing the glutamate molecules that reach its surface, serving as both a "vacuum" and a buffer (Tzingounis and Wadiche, 2007). Based on this evidence, as first approximation, we will consider the astrocyte as the vertical part of the absorbing boundary in Fig 4.

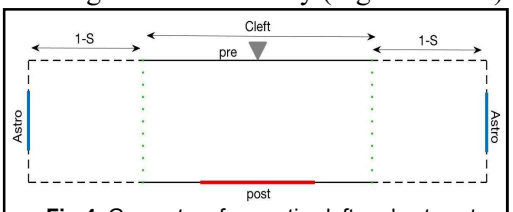

Fig 4. Geometry of synaptic cleft and astrocyte. Ensheathment determines box size 1-S.

As reviewed in Section 2, the astrocyte surface also contains glutamate receptors (blue bars in Fig.4). Their binding of glutamate starts a cascade of biochemical reactions, resulting in production of IP_3 and the calcium transient. The goal of this project component is to obtain a description of the astrocyte receptor activation time-courses and their dependence on S. We will also explore a possible role for different positioning of the receptors on the astrocyte surface. According to data from Wilcox lab, the location and density of receptors change during development and disease, but the implications of such change are unknown.

As a first step, we will find a spatial distribution of hits on the vertical boundaries of the synaptic box (Fig.4) for different values of ensheathment (i.e. different box sizes), including one with $S=S_c$, where the astrocyte fits exactly at the sides of the cleft (green lines). Once these distributions are known, and we make assumptions for locations of receptors, we will be able to compute the total number of particles that activate astrocyte receptors in the instantaneous case by integrating over the receptor locations.

In the case of receptors with non-instantaneous recharge, the total number of molecules captured or the astrocyte receptor activation time course can be thought of as a problem similar to the setup we considered

in Handy et al., (2018a,b) with one notable difference. All our previous results concerned delta-function initial condition for molecules release, both in space and time. If we consider astrocyte receptor in the same setting – with molecules entering its "box" opposite the receptor - the "initial condition" in this case corresponds to molecules crossing the green line (Fig.4) towards astrocyte. Thus, to be applicable, the theorems of Handy et al., (2018a,b) need to be generalized to this new spatially-extended initial condition.

Making an additional assumption that all molecules get deposited simultaneously, the initial condition reduces to the spatial distribution of molecules for $S=S_c$ above. Most of our proofs will carry through to this case, and we expect the necessary changes to be tractable. However, for the full time-course computation the molecules will continue to be deposited on the green line, and the analysis may become more challenging. We will collaborate with University of Utah probability group as before, to try to address the challenge, but will revert to simulations if needed. In any case, as a result of this project component we expect to have statistics of astrocyte receptor activation time course relating to different ensheathment values *S*, which will be used to generate inputs for the project component II.1.

4.2. Component II: Single synapse scale.

Rationale. Project components I.1 and I.2 described above will give us information about the time course and variability of post-synaptic and astrocyte receptor activation at different ensheathment levels. However, regulating glutamate levels in the synaptic cleft is only one of the ways astrocytes can influence nearby neurons. As described in Section 2.2, proximity of astrocyte to the synapse can also produce slowly changing ionic concentrations in the small space around the synapse and thus potentially modulate ionic reversal potentials, resting potential, and excitability of the postsynaptic neuron. Here, we set out to investigate how calcium activity (omnipresent in astrocytes, on time scale of seconds to minutes) may be modulating excitability of nearby neurons. The degree of ensheathment is expected to play a major role in the pathway from astrocyte calcium to neural excitability, as increased synaptic ensheathment restricts extracellular space and ionic concentration changes become easier to enact.

In project **Component II.1** we will use existing models and new results from I.2 to investigate statistics of astrocyte calcium responses as a function of the ensheathment parameter. In project **Component II.2** we will create a detailed model of tripartite synapse and model directly the pathway from astrocyte calcium activity to changes in extracellular ion concentrations and resulting reversal potentials (please, refer back to Fig.1 for a reminder of how different project components fit together).

Proposed work.

Component II.1. From astrocyte receptors activation to IP_3 and calcium response. As Component I.1 above, this project component is smaller and well-defined, and thus provides a good opportunity for an REU project. The student would be expected to have some background in programming and statistics, and will have the opportunity to gain further experience in both, while contributing to a larger research effort.

Our recent model of astrocyte calcium transients (Handy *et al.*, 2017; Taheri *et al.*, 2017) use time course of a signal molecule IP_3 as the input. To connect the result of project Component I.2 – dependence of astrocyte receptors activation on ensheathment – to the calcium response, we need an additional link connecting a time course of astrocyte receptors activation to a time course of IP_3. An existing model of De Pittà *et al.* (2009) provides such a link.

The work for this component will go in several steps: (i) Fix *S*. Using results of Component I.2 generate astrocyte receptors activation time course; (ii) Feed the receptors activation into the De Pittà *et al.* (2009) model, and record resulting $IP_3(t)$; (iii) Use $IP_3(t)$ as the input into our calcium response model, and record $Ca^{2+}(t)$. After this data is collected for multiple trials and at different values of *S*, the statistics of IP_3 and calcium time courses can be analyzed (rise and decay times, amplitude, duration, type of calcium response).

The resulting statistics can be compared to previously-generated artificial dataset and data from our collaborators (Taheri *et al*., 2017) and added to the database described in Section 3.1 above.

Component II.2. From astrocyte calcium to extracellular ion concentrations and neuron excitability.

In our previous work (Section 3.1), we created a detailed model of evoked calcium transients in astrocytes. Using this as a starting point, we would include key potassium and sodium fluxes, and begin to examine the level of calcium activity needed to have a significant impact on extracellular concentrations, and hence, the excitability of nearby neurons. While proposed experimentally, a detailed model including all three of these ions has not been created. Both extracellular Na^+ and K^+ concentrations may be influenced by astrocyte calcium transients through the following pathway: calcium transients drive the sodium-calcium exchanger (NCX) to pump Na^+ into the cell, which activates sodium-potassium pump (NKA) to pump this new Na^+ back out and, in return, K^+ is pumped in and extracellular K^+ decreases briefly. We propose to zoom out from our previous project components and consider a multi-compartment (extracellular space, astrocyte cytosol, and astrocyte ER) model of the tripartite synapse. While space is not included explicitly, the role of synaptic ensheathment can be investigated through the relative volumes of each compartment.

Fig. 5 shows the summary of the principal model components we will include. The left part of the astrocyte shows in a red dashed frame a summary of our existing calcium dynamics model (Handy *et al.*, 2017; Taheri *et al.*, 2017), and on the right are components that we will add. These include sodium-calcium exchanger (NCX), sodium-potassium pump (NKA), glutamate transporter (GLT) that also co-transports Na^+ and K^+, inward-rectifying K^+ channel (Kir4.1) and leak currents.

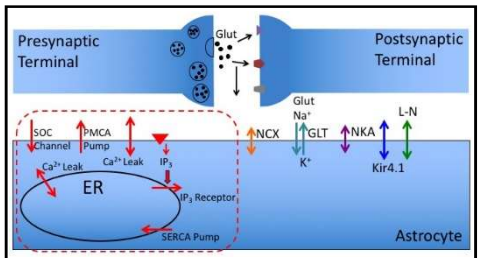

Fig 5. Extended tripartite synapse + Calcium

This study will proceed in 5 stages: (i) developing astrocyte-specific models for individual channels/pumps (Fig. 5) to add to the calcium dynamics model; (ii) parameter tuning to match basic astrocyte properties: behavior at rest, and intact basic glutamate-induced calcium dynamics, as in our original model; (iii) with a combination of analytical and numerical approaches, exploring the parameter space of relative strengths of new channel/pumps and the resulting effect on neuron excitability in a 1-synapse paradigm; (iv) fixing relative-strength parameters, explore the effect of varying the ensheathment parameter S in a 1-synapse paradigm; (v) studying the effect of varying the ensheathment parameter S in a simplified all-on-one network. For each of the stages we will maintain a close contact with astrocyte experts in Wilcox and White labs (see Letters of Collaboration) to discuss the model choices and assumptions that we will be making.

Stage (i) will require developing models for each of the fluxes listed in the right part of Fig. 5. We will keep each model as astrocyte-specific as the available data will allow, including kinetic parameters for each of the fluxes. For NCX, after a preliminary study (below) we have chosen to use a model from (Gall and Susa, 1999). While not fitted to astrocytes specifically, the model has all of the necessary characteristics found in the astrocyte data (Verkhratsky et al, 2012). Namely, it allows for the exchanger to run in reverse, and it depends on extra- and intracellular concentrations of Na^+ and Ca^{2+}, as well as the membrane potential. NKA models, in general, do not have much variation, so we have chosen to follow (Huguet *et al.*, 2016). We have tested existing model of Kir4.1 (Somjen *et al.*, 2008); Sibille *et al.*, 2014) against published data, and found that it needs to be refitted. We will have astrocytic current-voltage relationships from collected in the Wilcox lab, and will refit the model to them. For the GLT we will start with the detailed model of (Diamond, 2005), but will look for model reduction approaches, starting with the fast-slow reductions.

Once all model components are in place, in stage (ii) the main parameters to tune will be the strengths of the components relative to the calcium mechanisms, similar to the Preliminary Results below. Resting astrocyte characteristics (resting voltage and ion concentrations) and the intact original calcium dynamics

will serve as benchmarks. We will use a combination of bifurcation analysis (similar to what we have done in work described in Sec. 3.1), numerical simulations and a new uncertainty quantification method being developed in the PI's group (Viertel and Borisyuk, 2018) for constraining the parameter space. The new method is an extension the Multi-Element Probabilistic Collocation Method (Sindi *et al.*, 2009). As the original, the new method allows to study the parameter sensitivity of the model, but it also quantifies the extent to which each response characteristic (resting voltage, calcium response duration, etc.) is controlled by each of the new model currents. Based on this analysis, at the end of this stage we will have constrained the space of parameters, and also divided it into regions of similar dynamics.

For stages (iii) and (iv) we will use a 1-synapse paradigm. Consider a tripartite synapse, as in Fig. 5. Make the presynaptic neuron spike continuously at a low firing rate so that the post-synaptic potential (but not the astrocytic effects) will have decayed when the new input arrives. In part (iii) we will then characterize numerically the effect of the full tri-partite synapse on the postsynaptic neuron characteristics, such as the reversal potentials and leak parameters. We expect that they will be modulated on the astrocytic time scale (seconds to minutes), and slowly converge to an equilibrium. If there is no convergence, then the influence of astrocyte on the postsynaptic cell is even more complex than anticipated. In that case, we will treat reversal potentials in the network as slowly modulated variables instead of parameters, and make necessary adjustments in the rest of the project. In stage (iv) we will study the effect of varying the ensheathment S. We expect to obtain resulting reversal potentials and leak parameters for each value of S from 0 (no ensheathment) to 1 (maximal ensheathment).

Finally, as a first step towards understanding networks, we will consider multiple spiking presynaptic cells, all converging onto one postsynaptic cell, with the same synaptic strength and synaptic ensheathment parameter S, and characterize post-synaptic spiking as a function of S.

Preliminary results. We created a partial version of the model proposed here with a help of a summer REU student Daniel Griffin. He started with our model from Handy *et al.* (2017), and extended it to include sodium-calcium exchangers, sodium-potassium pumps, and leaky sodium and potassium channels. This initial attempt at extending the model did not focus on building these new components from astrocyte literature, but instead, we chose them from existing models, regardless of cell type, and investigated whether our hypothesized pathway is capable of creating meaningful change in the firing of neurons.

Additional effort was put into choosing a model for the sodium-calcium exchanger. While it is common to assume that this exchanger extrudes calcium into extracellular space in exchange for sodium, it has been shown in the astrocyte literature to also run in reverse (Verkhratsky *et al.*, 2012). As a result, we investigated models of the NCX from a couple of sources (Courtemanche *et al.*, 1998; Gall and Susa, 1999) to capture this important property, and have chosen to go with the latter one. This REU project also included a preliminary investigation of the relative strengths of the new and existing ion fluxes. We successfully tuned parameters of the model in such a way that our original calcium mode results remained entirely intact.

Further, we tested whether this pathway was strong enough to affect the firing of neurons. We created an artificial spike in extracellular potassium, and ran the model with and without a simultaneous calcium transient in the astrocyte. In the baseline condition (no potassium spike, no astrocyte activity) the step-current input to the neuron was not strong enough to make it fire (green line in Fig. 6, mostly overlaid with red). With the increased potassium and no astrocyte response the neuron did fire a spike (blue), but with the simultaneous calcium activity in the astrocyte, the potassium concentration was compensated, and the neuron returned to its original response (red). These preliminary results confirm astrocytes' ability to modulate spiking.

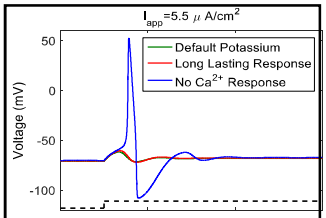

Fig 6. Neuronal spike with and without astrocyte Ca

4.3. Component III: Network scale.

Rationale. Even with a full understanding of the dynamics of a single tripartite synapse, it is not clear how these dynamics affect network level properties such as firing rate and synchrony. The connection between neuronal network structure and its firing properties has received much recent attention (e.g., de la Rocha *et al.*, 2007; Trousdale *et al.*, 2012; Rosenbaum *et al.*, 2017), but this field has been almost entirely devoid of astrocytes. In reality, as reviewed in section 2.3, different parts of the brain have different synaptic ensheathment distributions, and the role of such differences is unknown. There is also evidence that the degree of ensheathment may be altered in epileptic and other disease states (reviewed in Sec. 2). Partly this is due to astrocytes becoming reactive in a disease – this is a state that includes increased astrocyte volume.

In the third component of the project, we propose to develop a new type of neuronal network that includes the effects of astrocytes, without explicitly modeling astrocytes themselves (**Component III.1**). On one hand, the specific ways of incorporating the "effective astrocytes" will be derived based on our detailed studies in Components I and II, and thus will retain plausible accuracy. On the other, our approach, starting with networks of idealized neurons, and adding astrocytes only in the form of adjusted parameters of the network units, keeps the model tractable and amenable to analysis. We want to provide researchers with a way to include the effect of astrocytes in their existing networks with minimal adjustments.

Unlike previous work on heterogeneous networks, which usually consider relatively small variations in parameters, we expect a much higher degree of heterogeneity in the astro-neural network we are considering. Due to the novelty of this setup, we need to extend existing theory to include this increase in complexity to develop a robust understanding of how astrocyte ensheathment affects network behavior (general excitability, spiking patterns and synchronization). Specifically, in project **Component III.2** we plan to extend analytical results of Rosenbaum *et al.* (2017) to this new type of network under certain assumptions, and supplement it with numerical simulations under more general conditions, to find relation between astrocyte ensheathment levels, connectivity patterns and network's ability to synchronize.

Proposed Work.

Component III.1. Astro-neuronal network. We will start with one-layer recurrent network of excitatory and inhibitory exponential integrate-and-fire (EIF) units. Each neuron will send out a fixed number of connections, and each target will be chosen with replacement, with probability and connection strength decaying with distance (Fig 7A, top layer).

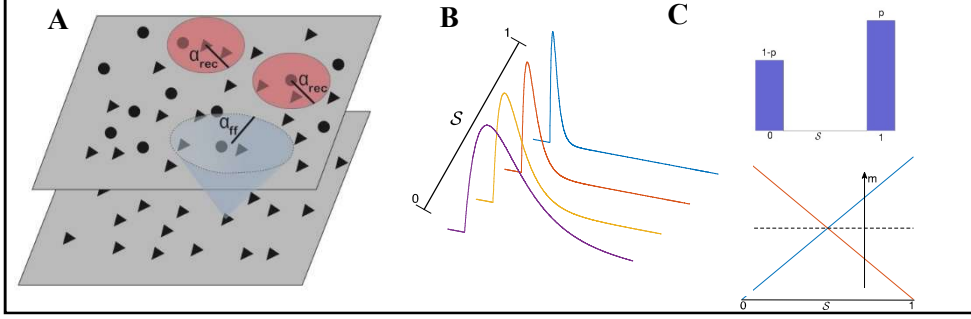

Fig 7. Proposed network model. *A*: two-layer network. *B*: A schematic of possible PSC dependence on the synaptic ensheathment parameter S. *C*: Distributions of S values that will be considered – binary (top) and linear with various slopes (bottom)

Next, each synapse in the network will be assigned its synaptic ensheathment parameter S_{ijk}, $0 \le S_{ijk} \le 1$, (for synapse number k between cells i and j). Once the values of S are chosen, the result of the project Component I.1 will allow to determine the unitary synaptic conductance for that synapse based on its S (Fig. 7B). The value of S will also determine how that synapse locally contributes to the excitability of the postsynaptic neuron (Component II.2). The overall excitability of each neuron (resting potential V_L^j and the time constant for spike generating currents of the EIF model Δ_T^j) will be determined individually by averaging "excitability contributions" over all its incoming connections. The resulting equations will be:

$$C_m \frac{dV_j}{dt} = I_L\left(V_j; V_L^j\right) + f\left(V_j; \Delta_T^j, g_L, V_T^j\right) + \sum_{i,k} w_{ijk} \cdot \left(\eta_i * \alpha_{S_{ijk}}\right)(t),$$

where f determines the EIF dynamics $f(V) = g_L \Delta_T^j \exp[(V - V_T)/\Delta_T^j]$; $\eta_i(t)$ is the spike train of neuron i; $\alpha_{S_{ijk}}(t)$ is the synaptic time course, and $*$ denotes convolution.

Values of S_{ijk} will be chosen from a distribution $P_S(x;\theta)$ parametrized by a parameter θ. Initially, we will take $P_S(x;\theta)$ to be Bernoulli, taking values 1 with probability p, and 0 with probability 1-p, and parametrized by $\theta = p$ (Fig 7C, top). This corresponds to fraction p of synapses being ensheathed to a maximal level, and the rest non-ensheathed. More generally, we will choose $P_S(x;\theta)$ to be a "trapezoidal" distribution family (Fig. 7C, bottom), where the density function is linear on [0,1], the parameter $\theta = m$ is the slope of the line, and it can vary from the highest probability located at 0 to the highest probability located at 1. In the next project component we will develop theory to find the parameter ranges where the asynchronous state can be supported, supplementing theory with numerical sim ulations where necessary.

Component III.2. Changes in network synchronizability with synaptic ensheathment. A recent paper (Rosenbaum *et al.*, 2017) investigated the role of local circuit architecture on correlated firing behavior, and how it influences the ability for a network to support an asynchronous state. Their conclusions rely on previously derived mean field theory of firing rates in balanced networks, as well as a newly developed cross-spectra measure of covariability. Specifically, they use the scaling properties of cross-spectral (Fourier transform of cross-correlation) matrices in an asynchronous state and the large network limit to derive their analytical conditions. While not a focus of their work, they also showed that their calculations are generalizable to heterogeneous networks with more than two subpopulations. While the results are general, they do rely on the assumption that the neurons are statistically identical in each subpopulation.

Our goal is to follow and extend the analysis of Rosenbaum *et al.* (2017) to compute analytically coherence and synchronization measures in a new network formalism that accounts for astrocytic ensheathment, and identify the parameter ranges where the network is able or unable to support asynchronous state.

Motivated by hippocampal CA3-CA1 network, we consider a two-layer arrangement, with a feedforward layer of excitatory neurons, and a recurrent excitatory-inhibitory layer (Fig. 7A). Rosenbaum *et al.* (2017) consider the same setup, but we allow for heterogeneity at each synapse and neuron as explained above.

We start the extension of theory by first assuming that all presynaptic terminals from neuron i have the same level of ensheathment, and that only the synaptic, but not intrinsic neuronal, parameters are affected by changes in ensheathment, because the mean field analysis employed in Rosenbaum et al. (2017) relies on homogeneity of the intrinsic properties of neurons. Under this assumption, all neurons are divided into $2N_S$ subtypes, where N_S is the number of synaptic ensheathment values that are considered, plus each neuron is characterized as excitatory or inhibitory. This reduces the heterogeneity in the network to a generalization of the usual excitatory-inhibitory case. For example, when S only takes values 0 and 1, we will have 4 neuron classes: (E,0), (E,1), (I,0), (I,1). Similar situation (but different in origin) was considered in Rosenbaum *et al.* (2017). Thus this extension of theory should be straightforward and it should yield interpretable results that match well with simulations.

For the next step, we will then allow for the outgoing synapses to vary in terms of their ensheathment parameter, still keeping the neuron's intrinsic properties ensheathment-independent. In order to analyze this much more heterogeneous network, we will first homogenize each neuron, by averaging ensheathment over its outgoing synapses, and then treating each of the synapses as the same. This will allow us to still consider subpopulation of neurons, though many more than in our previous step (if each neuron sends out K connections, and S only takes values of 0 and 1, there will be $(K+1)$ subpopulations). As a result, we can

apply similar theory from the previous; however, it is no longer clear whether the theory will yield results similar to simulations. The homogenization step will require thoughtful approximations, but even in the base case scenario, information about the network will be lost. We plan on deriving conditions where such a technique will yield mean-field results that are consistent with simulations. Finally, we expect direct simulations to be the most effective tool in study of fully heterogeneous networks, with both synaptic and intrinsic properties affected by the synaptic ensheathment.

To interpret possible results for each network modification, we recall that the distribution of S values that is heavier towards one (higher m) makes the network more similar to that in a disease state. If such networks are better at supporting asynchrony (and thus keeping the activity away from synchronized seizure activity), we would predict that the increased synaptic ensheathment in disease is likely playing a compensatory role. If, conversely, higher m makes the network more likely to synchronize, then we would predict that the increased synaptic ensheathment is likely contributing to the pathological manifestations of the disease.

5. BROADER IMPACT.

The results of this project will provide a novel point of view on a very general question of collective activity in neuronal networks. The inclusion of astrocytes in networks in a detailed, principled way will generate insights of great interest to the computational neuroscience community. This work will have substantial impact in understanding the role of astrocytes in the brain in many different conditions, including diseases related to astrocyte dysfunction. The resulting models will comprise important parts of computational neuroscience courses taught at Utah. This project will also have an educational impact beyond the computational neuroscience community. The PI teaches mathematical biology courses at all possible levels and to diverse audiences including mathematicians, biologists, engineers, and pre-medical students.

Results of the project will be presented at national and international conferences and workshops. The resulting software will be made publicly available through ModelDB and on the PI's website.

Graduate students recruited for this project will be involved in all phases of model development, theory and analysis. They will be able to interact with both mathematical and biological collaborators, acquiring skills for conducting interdisciplinary research. They will also be able to participate in courses, journal clubs, seminars and workshops at University of Utah (including those funded by Math Bio NSF RTG program).

The PI will continue her educational efforts, including undergraduate and graduate colloquia, and efforts to attract underrepresented groups to STEM fields. As the Director of Undergraduate Studies in her department she is involved in all aspects of the undergraduate education and research advancement.

In her outreach activities, Borisyuk participates in K-12 teacher training in interdisciplinary thinking. She has also been the leader and organizer of the Math Circle for elementary students for the past 4 years. She has also been teaching and mentoring students in the ACCESS program – a summer program for women entering university with STEM interests.

The PI's group also has very good track records of working with undergraduates and mentoring students from diverse backgrounds. Just over the last 2 years her group has hosted 5 undergraduate research projects (including 3 women, 2 minority students) and a high school student. She also has graduate students from underrepresented groups, including first-generation college student. Members of the PI's group are also encouraged to get involved in various educational and outreach efforts themselves. They have recently participated in the Science Day (STEM open house day), were involved with Splore, a non-profit organization that specializes in accessible outdoor adventures through STEM Ambassador NSF-funded program (STEMAP; http://www.stemap.org), and took part in development of new precalculus materials.